

## Parallel Polarization EPR Characterization of the Mn(III) Center of Oxidized Manganese Superoxide Dismutase

Kristy A. Campbell,<sup>†</sup> Emine Yikilmaz,<sup>‡</sup> Christopher V. Grant,<sup>†</sup> Wolfgang Gregor,<sup>†</sup> Anne-Frances Miller,<sup>\*,‡</sup> and R. David Britt<sup>\*,†</sup>

Department of Chemistry, University of California  
Davis, California 95616

Departments of Chemistry and Biophysics  
The Johns Hopkins University, 3400 North Charles Street  
Baltimore, Maryland 21218

Received January 22, 1999

Revised Manuscript Received March 25, 1999

Manganese superoxide dismutase (MnSOD) is an enzyme found in mitochondria and chloroplasts of eukaryotes and in the cytoplasm of bacteria.<sup>1,2</sup> The redox active Mn ion cofactor catalyzes the one-electron redox cycle by a two-step disproportionation reaction with oxidized Mn<sup>3+</sup> in the resting state.

In this report, we have used parallel polarization CW-EPR to investigate the paramagnetic Mn<sup>3+</sup> ion of the MnSOD enzyme from *Escherichia coli* overexpressed from pALS1 in HMS174/DE3. The crystal structure of native MnSOD from *E. coli* has been determined to 2.1 Å resolution.<sup>3</sup> Crystal structures have also been solved for MnSOD of *Thermus thermophilus*<sup>4</sup> and human mitochondria.<sup>5</sup> These structures show high homology between the bacterial and the eukaryotic MnSOD and confirm that in each case the Mn<sup>3+</sup> ion has five ligands (three histidines, one aspartate, and one hydroxide ion) with a distorted trigonal-bipyramidal geometry. In this configuration, the d<sup>4</sup> Mn<sup>3+</sup> ion is high-spin with an effective total spin  $S = 2$ .<sup>6,7</sup>

The energy levels of an  $S = 2$  integer spin system with a positive axial zero-field splitting value,  $D$ , are arranged as shown in Figure 1. An EPR signal from the MnSOD Mn<sup>3+</sup> ion has not previously been detected with conventional X-band EPR methods.  $D$  is predicted to be more than 2 cm<sup>-1</sup> based on SQUID saturation magnetization studies of the oxidized form of native MnSOD,<sup>7</sup> or between 1–2 cm<sup>-1</sup> based on MCD studies.<sup>6</sup> Because of the large zero-field splitting values, the conventional perpendicular polarization EPR allowed  $\Delta M_s = \pm 1$  transitions are not possible at normal X-band microwave frequencies (0.3 cm<sup>-1</sup>) (See Figure 1). However, EPR signals from integer spin systems can be detected when the oscillating magnetic field applied to induce a spin-state transition is oriented parallel to the static magnetic field. The parallel magnetic field orientation allows transitions between the closely spaced  $M_s = \pm 2$  energy levels (Figure 1 inset), to be observed with signal intensities many orders of magnitude larger than the corresponding perpendicular magnetic field orientation.<sup>8</sup>

Figure 2a shows the parallel polarization EPR spectrum of the Mn<sup>3+</sup> ion of native MnSOD. This signal is centered at an effective

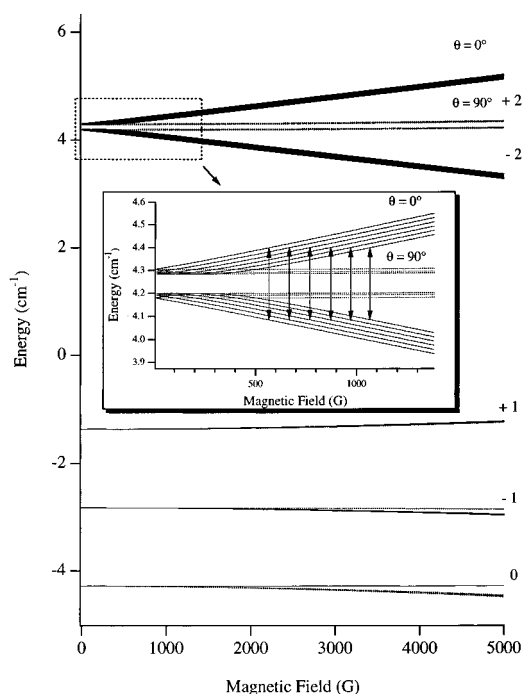


**Figure 1.** Energy level diagram of an  $S = 2$  spin system, obtained via eq 1 with matrix diagonalization, with  $D = 2.10 \text{ cm}^{-1}$ ,  $E = 0.243 \text{ cm}^{-1}$ ,  $A_x = A_y = 101 \text{ G}$ ,  $A_z = 100 \text{ G}$ ,  $g_x = 2.00$ ,  $g_y = 1.99$ ,  $g_z = 1.98$ , and  $\theta = 0^\circ$  and  $90^\circ$  with  $\phi = 0^\circ$ . The inset figure is an expanded view of the  $M_s = \pm 2$  energy levels in the region of the observed parallel mode EPR transitions of Figure 2 (indicated by arrows).

$g$  value of 8.17 and consists of six hyperfine lines separated by approximately 100 G. This EPR signal is absent in the conventional perpendicular mode spectrum (data not shown). The spin Hamiltonian describing this system is

$$\hat{H} = \beta_e \vec{B}_0 \cdot \vec{g}_e \cdot \hat{S} + D \left( \hat{S}_z^2 - \frac{1}{3} S(S+1) \right) + \frac{E}{2} (\hat{S}_+^2 + \hat{S}_-^2) + \hat{S} \cdot \vec{A} \cdot \hat{I} \quad (1)$$

where  $\beta_e$  is the electron Bohr magneton;  $\vec{B}_0$  is the static magnetic field vector;  $\vec{g}_e$  is the electron  $g$  tensor;  $\hat{S}$  is the electron spin operator (total spin  $S = 2$ );  $D$  is the axial zero-field splitting parameter;  $E$  is the rhombic zero-field splitting parameter;  $\vec{A}$  is the nuclear hyperfine tensor; and  $\hat{I}$  is the nuclear spin operator for the 100% abundant <sup>55</sup>Mn nucleus ( $I = 5/2$ ). The EPR spectrum in Figure 2a was simulated using the Hamiltonian in eq 2 and diagonalizing the corresponding  $30 \times 30$  Hamiltonian matrix for the  $S = 2$ ,  $I = 5/2$  system to determine the eigenvalues and eigenfunctions at a constant microwave frequency as a function of magnetic field. A Boltzmann distribution was included to account for the temperature dependence of the EPR signal. The transition probability was calculated with the applied oscillating field parallel to the static magnetic field and then multiplied by a Gaussian lineshape function. The resulting simulated spectrum was differentiated in order to compare with the experimental spectrum which was obtained with derivative mode CW-EPR. An excellent simulation, shown in Figure 2b, was obtained using zero-field splitting values  $D = 2.10 \text{ cm}^{-1}$  and  $E = 0.24 \text{ cm}^{-1}$ . No distribution of  $D$  or  $E$  parameters was required to simulate this highly hyperfine-resolved spectrum. The transitions giving rise to the EPR spectrum are shown in the inset figure of the energy level diagram in Figure 1 (marked by double-headed arrows). The observed EPR peaks correspond to the  $\theta = 0^\circ$

(9) van Veen, G. J. *Mag. Reson.* 1978, 30, 91–109.

<sup>†</sup> University of California.

<sup>‡</sup> The Johns Hopkins University.

(1) Christianson, D. W. *Structural Chemistry and Biology of Manganese Metalloenzymes*. *Prog. Biophys. Mol. Biol.* 1997, 67, 217–252.

(2) Miller, A.-F.; Sorkin, D. L. *Comments Mol. Cell. Biophys.* 1997, 9, 1–48.

(3) Edwards, R. A.; Baker, H. M.; Whittaker, M. M.; Whittaker, J. W.; Jameson, G. B.; Baker, E. N. *J. Biol. Inorg. Chem.* 1998, 3, 161–171.

(4) Ludwig, M. L.; Metzger, A. L.; Patridge, K. A.; Stallings, W. C. *J. Mol. Biol.* 1991, 219, 335–358.

(5) Borgstahl, G. E. O.; Parge, H. E.; Hickey, M. J.; Beyer, W. F.; Hallewell, R. A.; Tainer, J. A. *Cell* 1992, 71, 107–118.

(6) Whittaker, J. W.; Whittaker, M. M. *J. Am. Chem. Soc.* 1991, 113, 5528–5540.

(7) Peterson, J.; Fee, J. A.; Day, E. P. *Biochim. Biophys. Acta* 1991, 1079, 161–168.

(8) Abragam, A.; Bleaney, B. *Electron Paramagnetic Resonance of Transition Ions*; Oxford University Press: London, 1970.

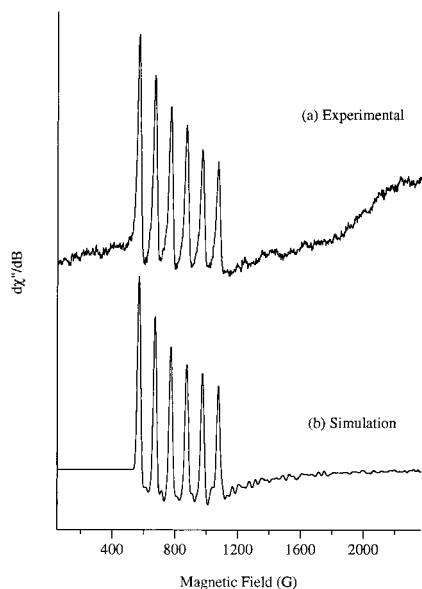


**Figure 2.** (a) Parallel mode CW-EPR spectrum of  $\text{Mn}^{3+}$  SOD. Experimental parameters are: microwave frequency, 9.41 GHz; microwave power, 32 mW; and temperature 10 K. (b) Derivative of the simulation of the experimental data. Simulation parameters are  $D = 2.10 \text{ cm}^{-1}$ ,  $E = 0.24 \text{ cm}^{-1}$ ,  $A_x = A_y = 101 \text{ G}$ ,  $A_z = 100 \text{ G}$ ,  $g_x = 2.00$ ,  $g_y = 1.99$ ,  $g_z = 1.98$ ,  $T = 10 \text{ K}$ , Gaussian linewidth parameter, 10 G. The powder pattern<sup>9</sup> was simulated with  $\theta = 0.1$  to  $89.7^\circ$ , 448 angles with  $0.2^\circ$  increments, and  $\phi = 0.1$  to  $88.1^\circ$ , 11 angles with  $8^\circ$  increments. Note, the "simulation noise" in the baseline of the simulation results from the finite number of angles selected for the powder pattern simulation. Sample conditions: 1 mM native MnSOD in 100 mM  $\text{H}_2\text{KPO}_4$ , 100 mM KBr, 40% glycerol, at pH 7.65.

("parallel") turning points and have absorption-like lineshapes because they are the derivatives of the rising edges of these powder patterns. As can be deduced from the energy level diagram, transitions are allowed well past the  $g = 2$  magnetic field region when  $\theta$  is varied from 0 to  $90^\circ$ . However, the distribution of angles in the powder pattern broadens the appearance of these transitions such that they do not result in well-localized peaks such as observed at low field for values of  $\theta$  close to  $0^\circ$ .<sup>10</sup>

Figure 3 shows the experimental temperature dependence of the native MnSOD parallel mode EPR signal, along with a theoretical simulation of the temperature-dependent data. The simulation of the temperature dependence of the parallel mode EPR signal was performed by varying the temperature parameter in the full diagonalization EPR simulation program. The experimental temperature dependence could be fit using a range of zero-field splitting values from  $D = 2.00$  to  $D = 2.15 \text{ cm}^{-1}$  with  $E = 0.24 \pm .01 \text{ cm}^{-1}$ . However, the closest fit to both the experimental temperature dependence and EPR spectrum was with  $D = 2.10 \text{ cm}^{-1}$  and  $E = 0.24 \text{ cm}^{-1}$ . The resulting temperature dependence fit and EPR spectrum fit confirms that the EPR signal arises from a transition between the  $M_s = \pm 2$  electron-spin states.<sup>11</sup> The EPR

(10) The perpendicular mode spectrum was simulated using the same parameters and shows signal amplitudes less than 1/1000 those of the parallel mode simulation, thus substantiating our choice of simulation parameters.

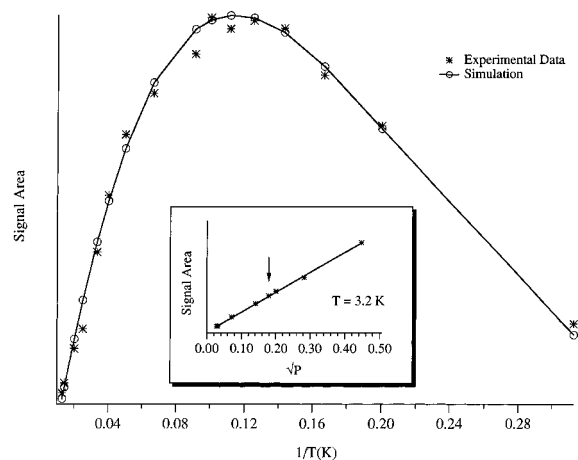


**Figure 3.** Experimental and theoretical temperature dependence of the EPR signal area vs  $1/T$  for  $D = 2.10 \text{ cm}^{-1}$  and  $E = 0.24 \text{ cm}^{-1}$ . Inset: power dependence (signal area vs  $\sqrt{P}$ ) of the EPR signal at 3.2 K; the arrow denotes the nonsaturating power (32 mW) used for the temperature-dependence measurements. Experimental conditions are the same as in Figure 2, except  $T$  which is varied for the temperature dependence plot and the power which is varied for the power-dependence plot.

spectrum can be simulated with  $D$  and  $E$  outside of the range reported here; however, in these cases the temperature dependence does not fit the experimental data.

Upon treatment of MnSOD with azide, a functional inhibitor, the six-line parallel mode CW-EPR signal disappears (data not shown). The  $\text{Mn}^{3+}$  ion geometry changes from 5-coordinate in the native sample to a 6-coordinate distorted octahedral geometry with azide forming the sixth ligand at temperatures below 200 K.<sup>12</sup> In addition, it is predicted on the basis of MCD studies<sup>6</sup> that  $D$  will become negative upon azide binding. The lack of an observed parallel mode CW-EPR spectrum in the temperature range of 3–70 K (data not shown) shows that indeed the zero-field splitting parameters are altered, indicating that parallel polarization EPR of the Mn(III) ion provides a sensitive probe of ligation.

Recently, with the observation of an integer spin EPR signal from the oxygen-evolving Mn cluster in photosystem II,<sup>13</sup> we have demonstrated that hyperfine-resolved spectra could be obtained on enzymatic Mn clusters. The MnSOD spectrum reported here demonstrates that this holds for monomeric Mn(III) enzymes as well.

**Acknowledgment.** We acknowledge the NSF (Grant MCB-9418181, A.F.M.) and the NIH (Grant GM48242, R.D.B.) for support of this work. A fellowship from the Department of Chemistry at UC Davis is gratefully acknowledged by K.A.C.

JA9902219

(11) Reif, F. *Statistical and Thermal Physics*; McGraw-Hill, Inc.: New York, 1965; Chapter 7.8.

(12) (a) Whittaker, M. M.; Whittaker, J. W. *Biochemistry* **1996**, *35*, 6762–6770. (b) Lah, M. S.; Dixon, M. M.; Patridge, K. A.; Stallings, W. C.; Fee, J. A.; Ludwig, M. L. *Biochemistry* **1995**, *34*, 1646–1660.

(13) (a) Campbell, K. A.; Peloquin, J. M.; Pham, D. P.; Debus, R. J.; and Britt, R. D. *J. Am. Chem. Soc.* **1998**, *120*, 447–448. (b) Campbell, K. A.; Gregor, W.; Pham, D. P.; Peloquin, J. M.; Debus, R. J.; Britt, R. D. *Biochemistry* **1998**, *37*, 5039–5045.